Liouville mapping predictions for quasi-perpendicular collisionless shocks

H. Comișel (ITP TUBS, ISS Bucharest)

in collaboration with
M. Scholer (MPE Garching)
O. Marghitu (ISS Bucharest)
Y. Narita (IWF Graz)
U. Motschmann (ITP TUBS)

▷ J.Geophys.Res. Vol. 112, A09212, 2007, "Electron dynamics and cross-shock potential at the quasi-perpendicular Earth's bow shock", B. Lefebfre, S.J. Schwartz, A.F. Fazakerly, P. Decreau

Vlasov equation: conservation of the phase space density along its characteristic

Gyrotropy of the electron distribution function and conservation of the magnetic moment $\mu = mv_\perp^2/2B = const$

Electron energy conservation in the de Hoffmann-Teller frame

$$\frac{mv_{\|1}^2}{2} + \mu_1 B_1 = \frac{mv_{\|2}^2}{2} + \mu_2 B_2 - e\Phi = const$$

$\vec{E} \times \vec{B} \sim 0$ through shock transition

Table 2. Summary of Main Shock Parameters at the Asymptotic Upstream and Downstream Locations[a]

Parameters	Units	19 December 2003 (u)	19 December 2003 (d)	23 January 2004 (u)	23 January 2004 (d)	19 March 2005 (u)	19 March 2005 (d)
B	nT	3.26	10.7	11.7	35.7	7.82	26.2
n_e	cm^{-3}	11	37.8	6.59	21.9	7.76	19.3
T_e	eV	14.3	25.8	22.8	90.8	17.2	70.8
$T_{e\|\|}/T_{e\perp}$	–	1.08	1.01	1.64	1.1	1.14	0.934
$T_{e\perp}/B$	eV/nT	4.3	2.40	1.60	2.46	2.10	2.76
T_p	eV	7.38	107.0	35.5	327	30.6	276
β_e	–	5.99	3.4	0.45	0.63	0.88	0.8
β_p	–	3.09	14.1	0.69	2.26	1.56	3.12
v_p	km/s	220	58.7	550	194	474	134
$\theta_{Bn,timing}$	deg	75.9	86.4	72	79.2	81.2	89.2
$\theta_{Bn,AS}$	deg	72.1	84.7	77.3	85.9	76.1	85.9
$\theta_{Bn,model}$	deg	70.3	81.4	75.6	84.7	72.6	82.9
Proton ram energy, $m_p u_p^2/2$	eV	253	18	1580	196	1170	94.2
Alfvén Mach number, M_A	–	10.3	1.54	5.56	1.16	7.76	1.03
Fast Mach number, M_f	–	4.22	0.787	4.79	0.946	5.96	0.801
HTF electron thermal Mach number, M^{I}_{Te}	–	0.402	0.309	0.627	0.183	1.26	1.97
Electron plasma frequency, f_{pe}	kHz	29.8	55.2	23.1	42	25	39.4
Electron gyrofrequency, f_{ge}	Hz	91.3	301	326	1000	219	734
Proton gyrofrequency, f_{gp}	Hz	0.0495	0.163	0.177	0.543	0.119	0.398
Electron inertial length, c/ω_{pe}	km	1.6	0.864	2.07	1.14	1.91	1.21
Thermal electron gyroradius, ρ_e	km	2.76	1.12	0.976	0.634	1.26	0.764
Proton inertial length, c/ω_{pp}	km	68.4	37	88.5	48.6	81.6	51.8
Thermal proton gyroradius, ρ_p	km	85	98.2	52.2	51.7	72.2	64.6
Convected proton gyroradius, v_{p1}/Ω_{cp}	km	707	215	494	161	636	190

▷ J.Geophys.Res. Vol. 112, A09212, 2007, "Electron dynamics and cross-shock potential at the quasi-perpendicular Earth's bow shock", B. Lefebfre, S.J. Schwartz, A.F. Fazakerly, P. Decreau

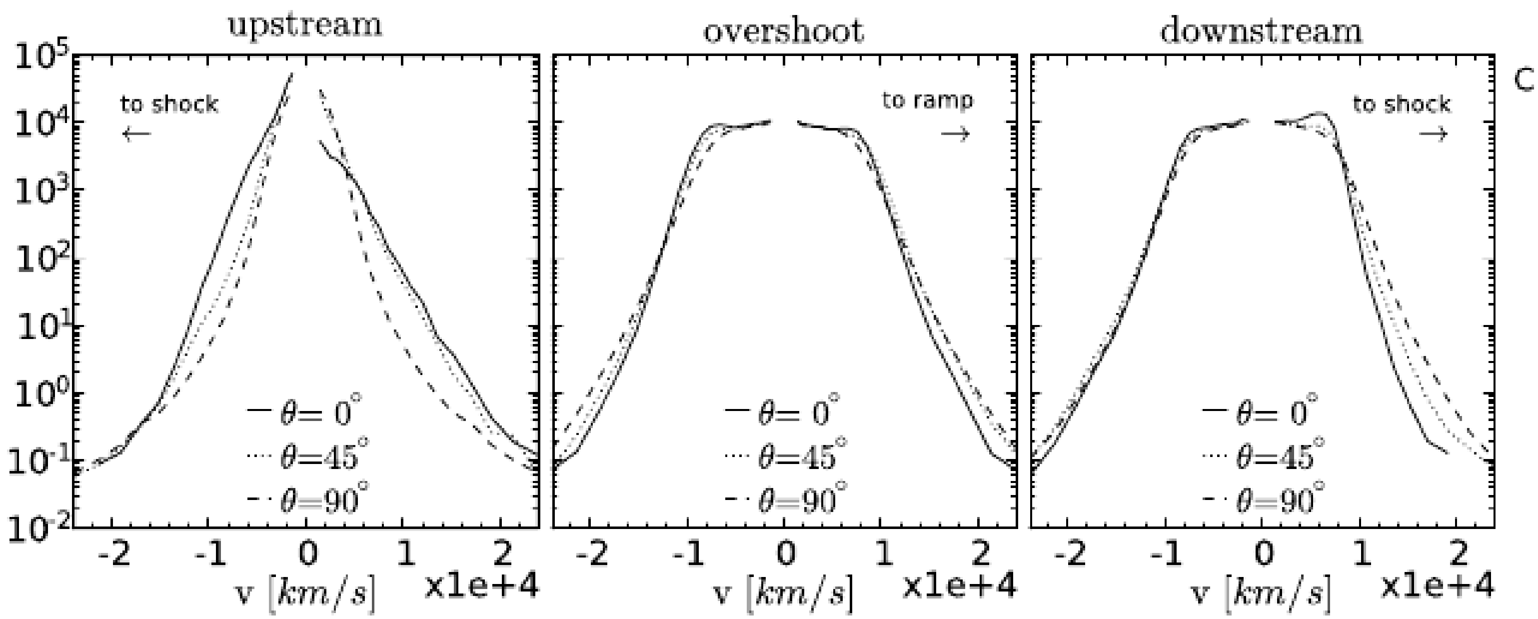

▷ J.Geophys.Res. Vol. 112, A09212, 2007, "Electron dynamics and cross-shock potential at the quasi-perpendicular Earth's bow shock", B. Lefebfre, S.J. Schwartz, A.F. Fazakerly, P. Decreau

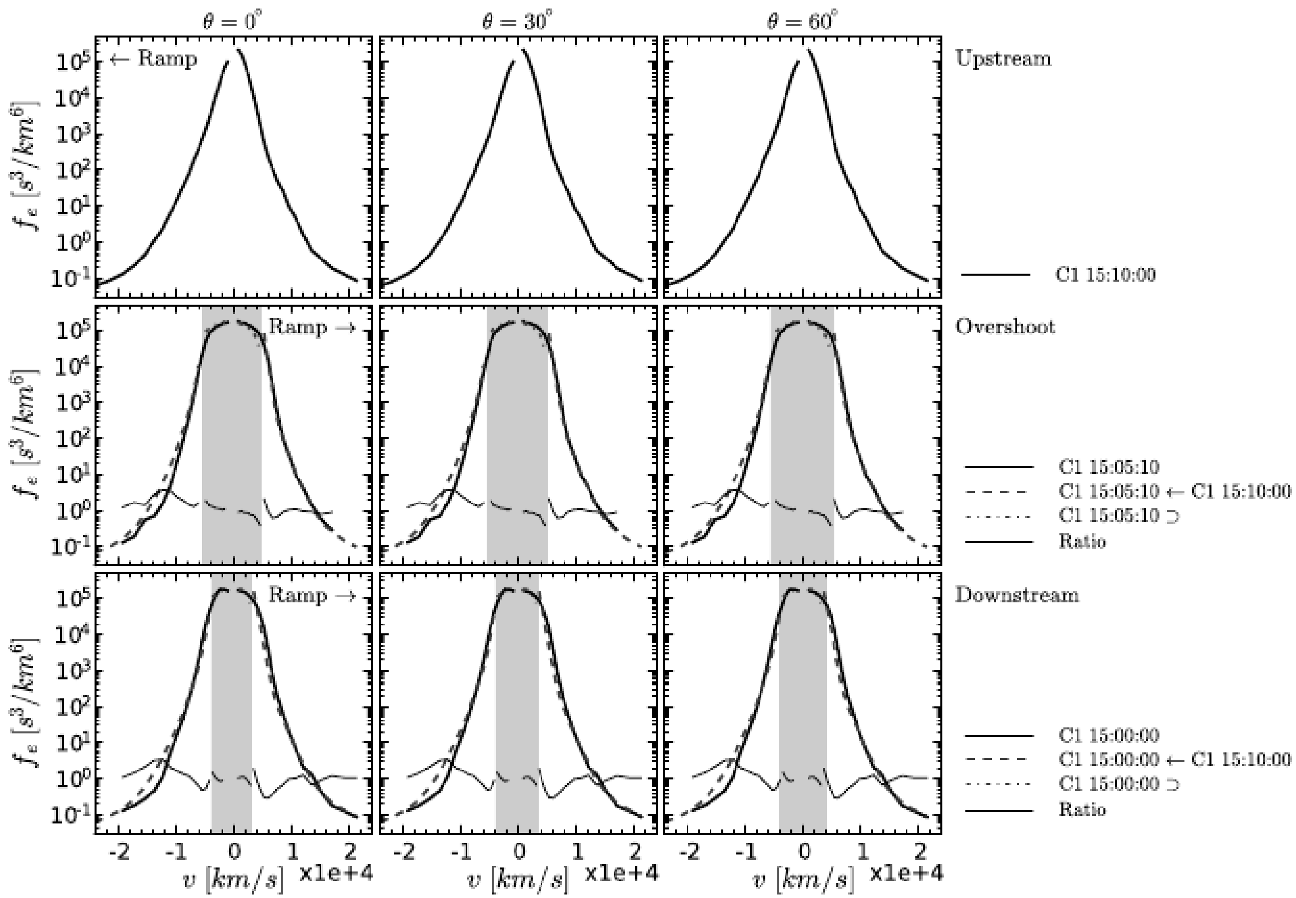

▷ J.Geophys.Res. Vol. 112, A09212, 2007, "Electron dynamics and cross-shock potential at the quasi-perpendicular Earth's bow shock", B. Lefebfre, S.J. Schwartz, A.F. Fazakerly, P. Decreau

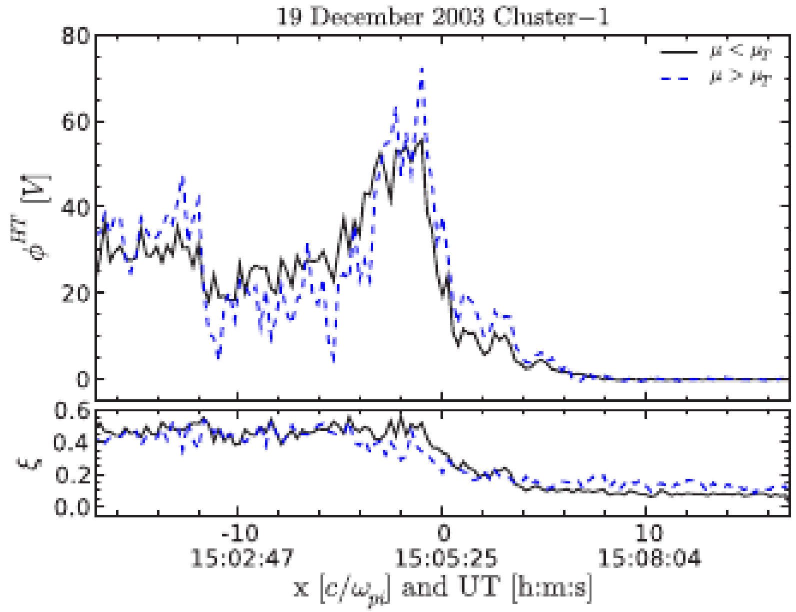

1-D PIC Simulation - Parameters

High Mach Number Bow Shock

M_A=10, θ=81^o, β_i=0.2, β_e=0.2

Number of cells: 40000

System size: 1581 λ_e (37 λ_i)

Number of particles/cell: 2 x 490

$\omega_{pe}^2/\omega_{ce}^2$=64

m_i/m_e= 1800

Magnetic field B_z stackplot

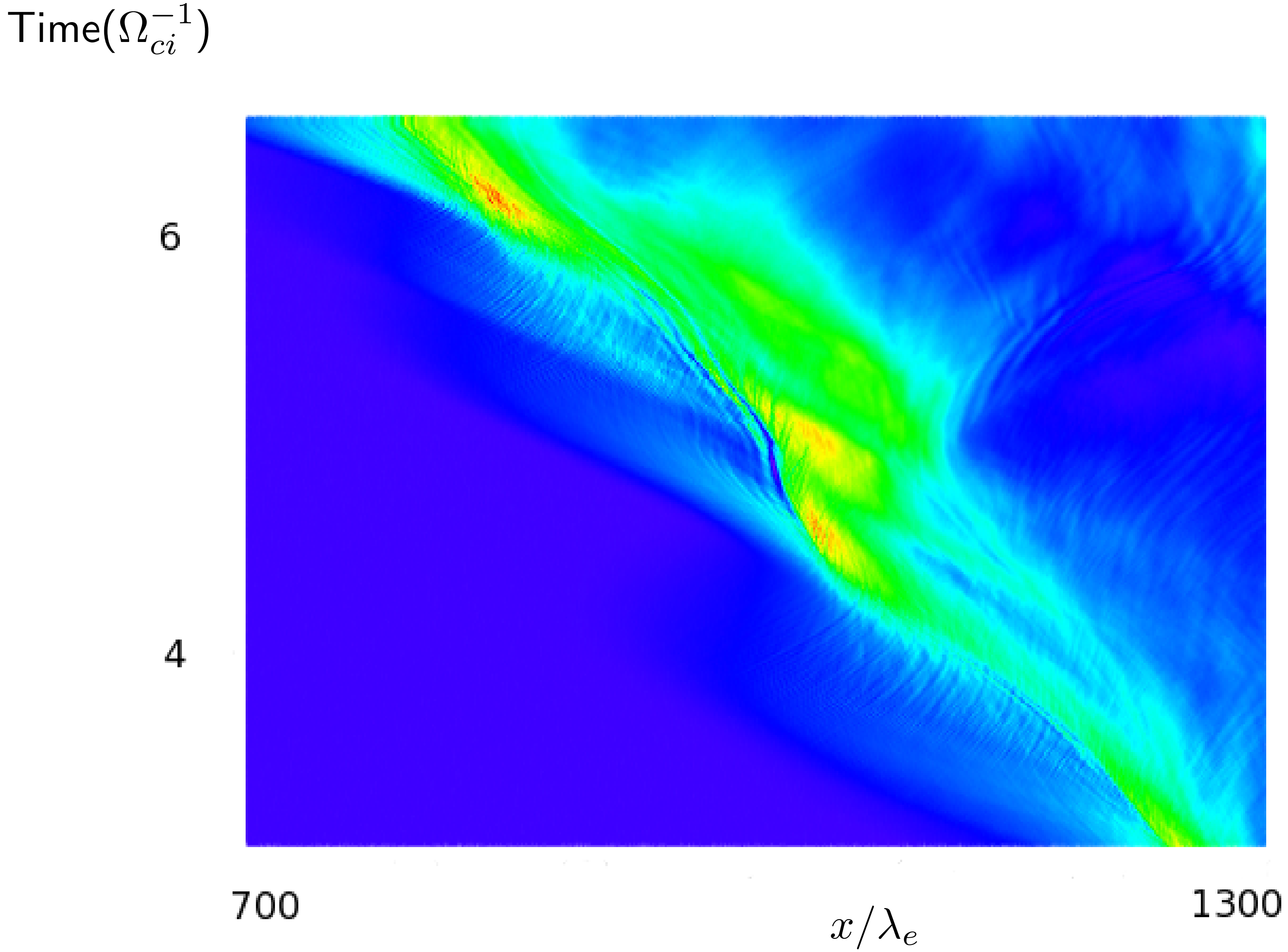

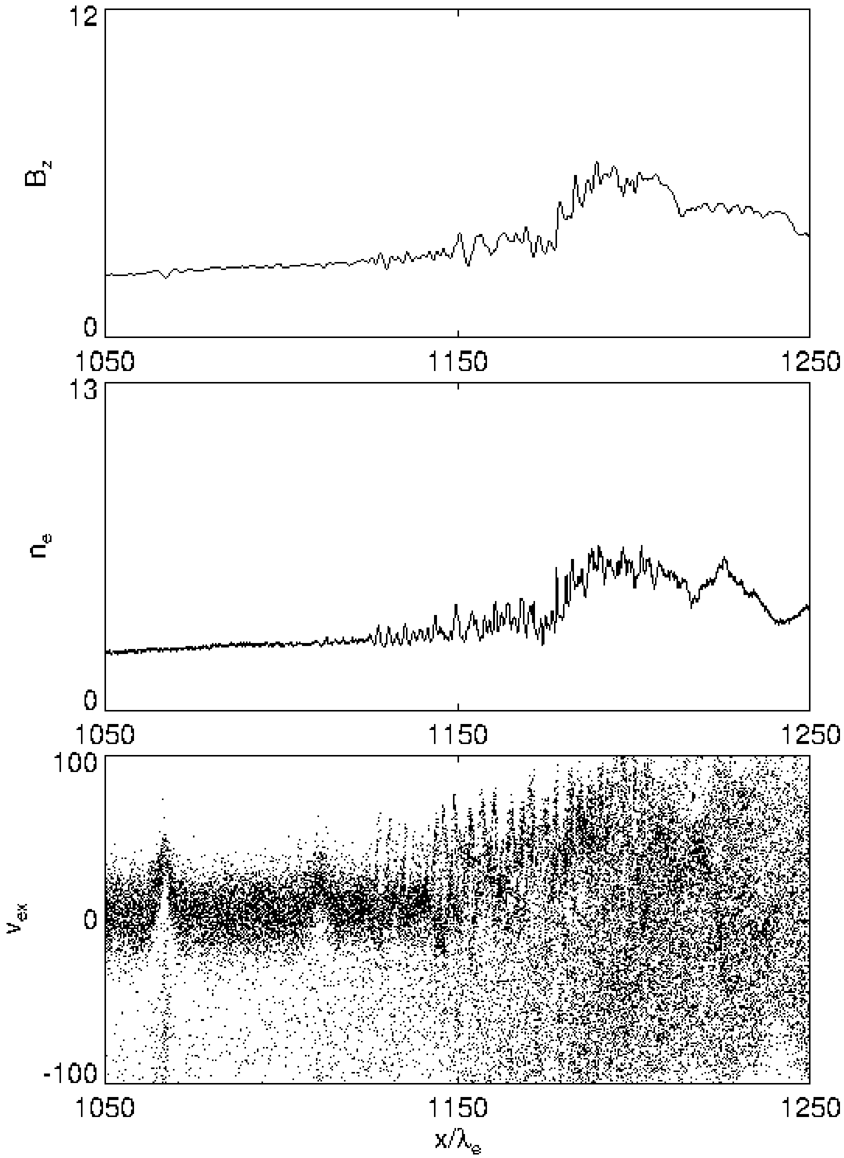

$T_1(\Omega_{ci}^{-1}) = 3.5$

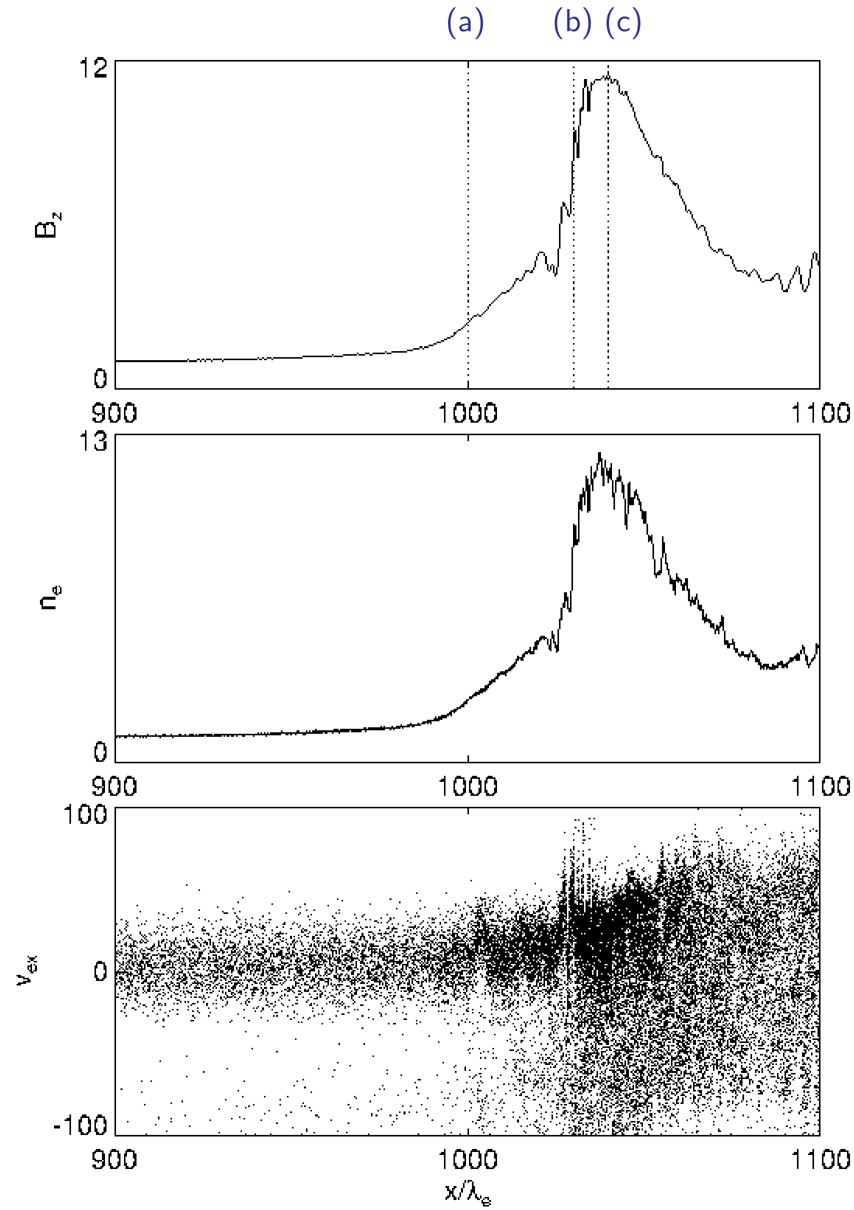

$T_2(\Omega_{ci}^{-1}) = 4.5$

Electron Phase Space Topology

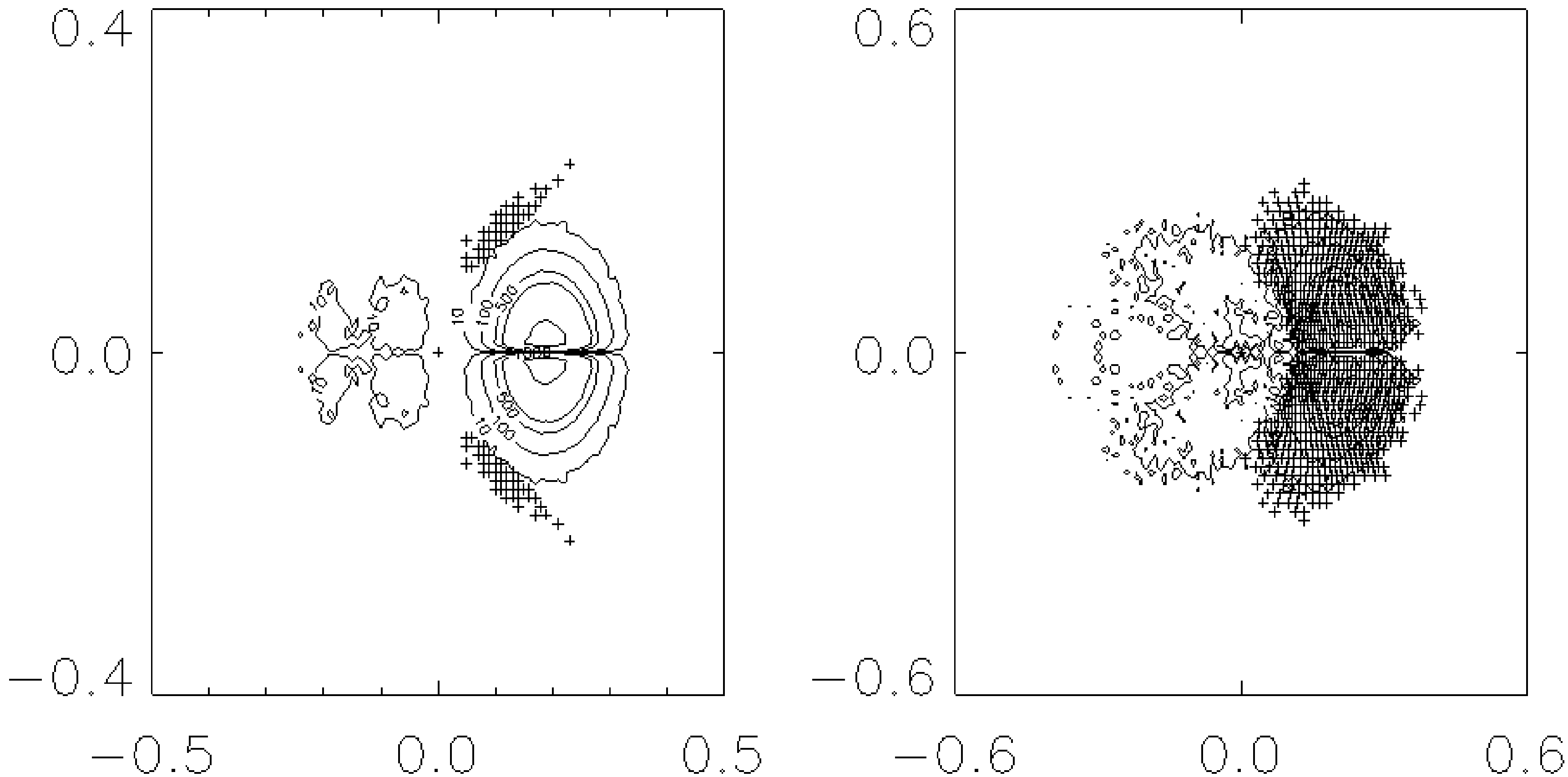

Cut (a)

Electron Phase Space Topology

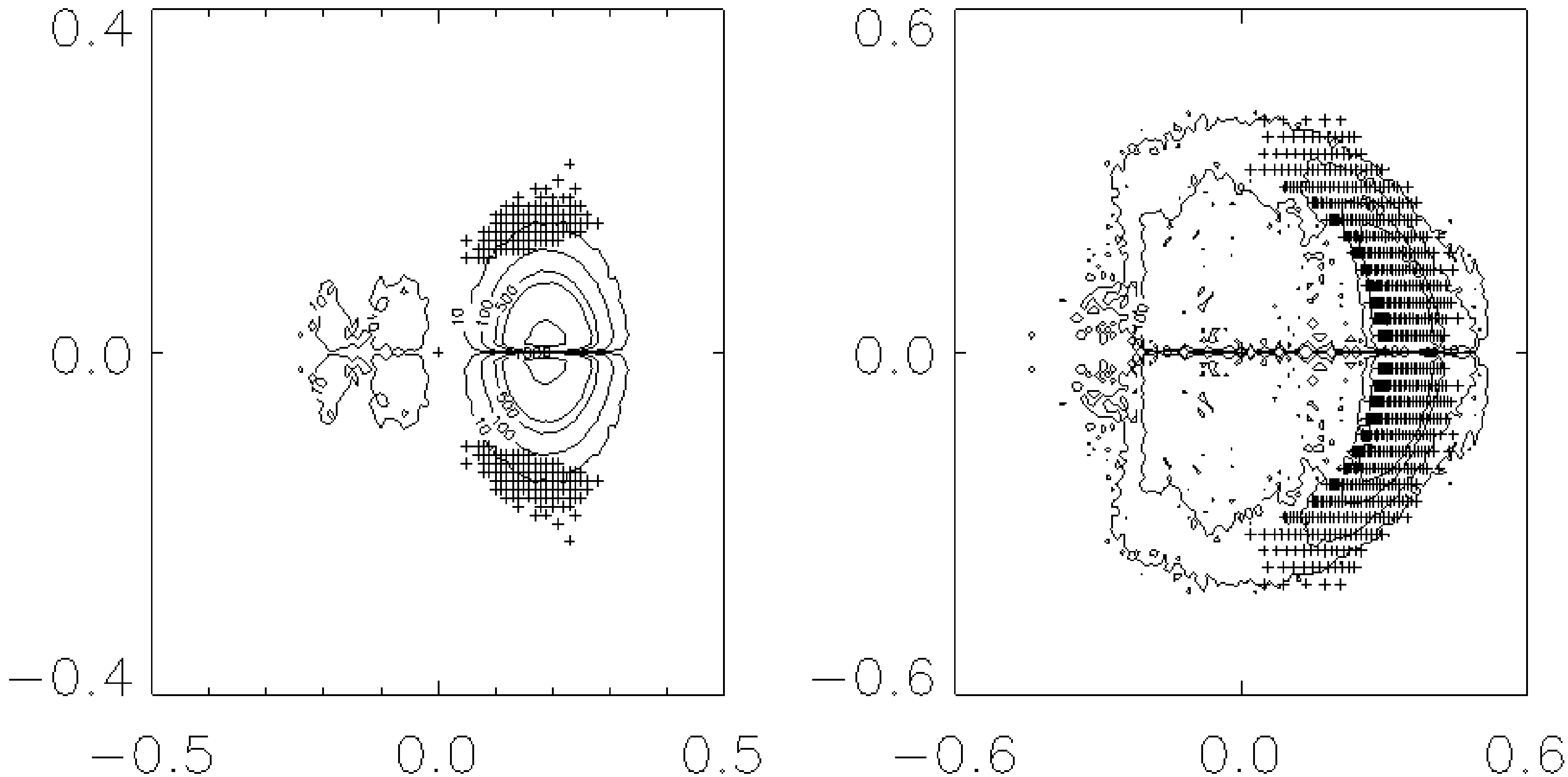

Cut (b)

Electron Phase Space Topology

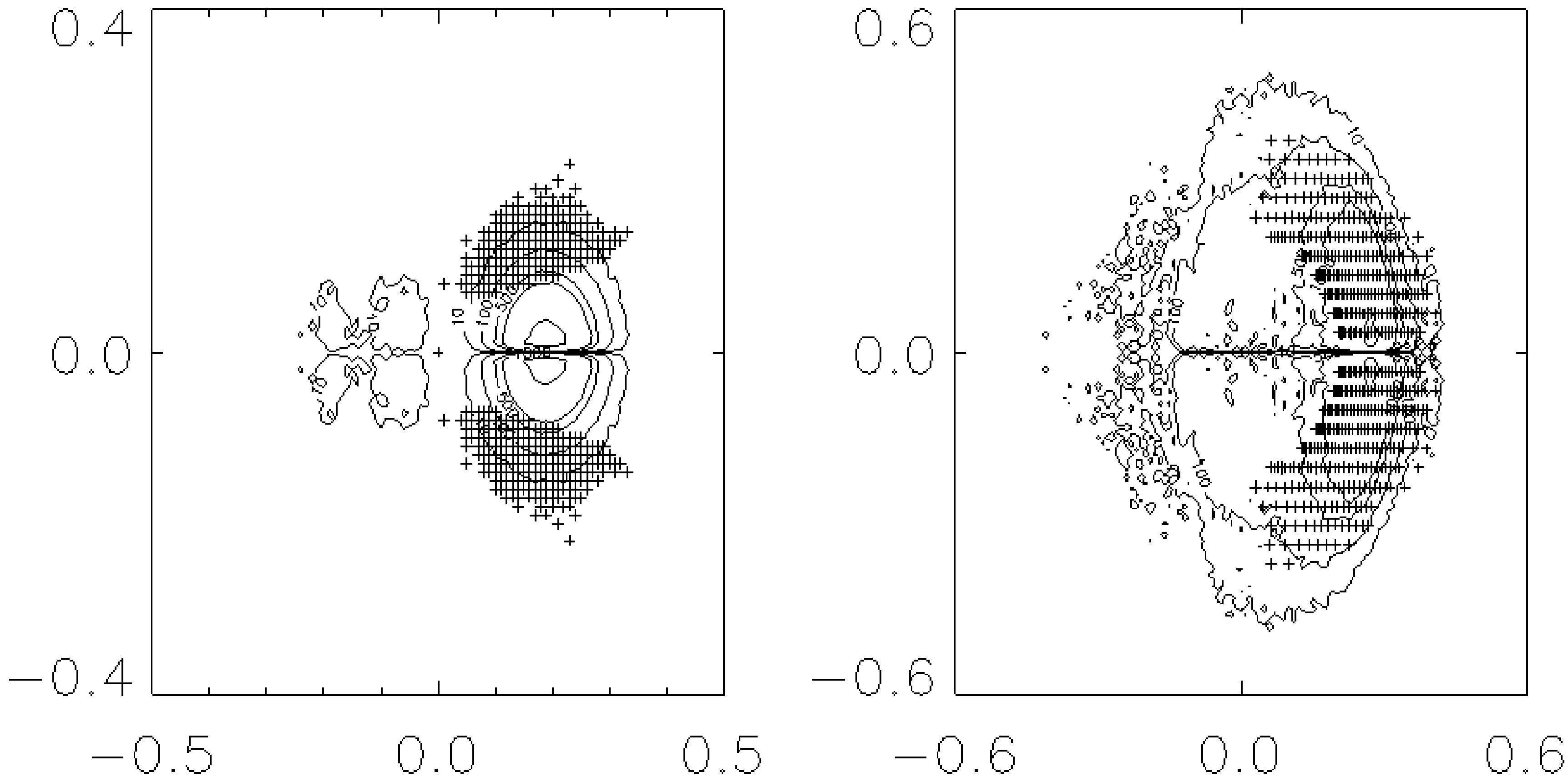

Cut (c)

Liouville Mapping

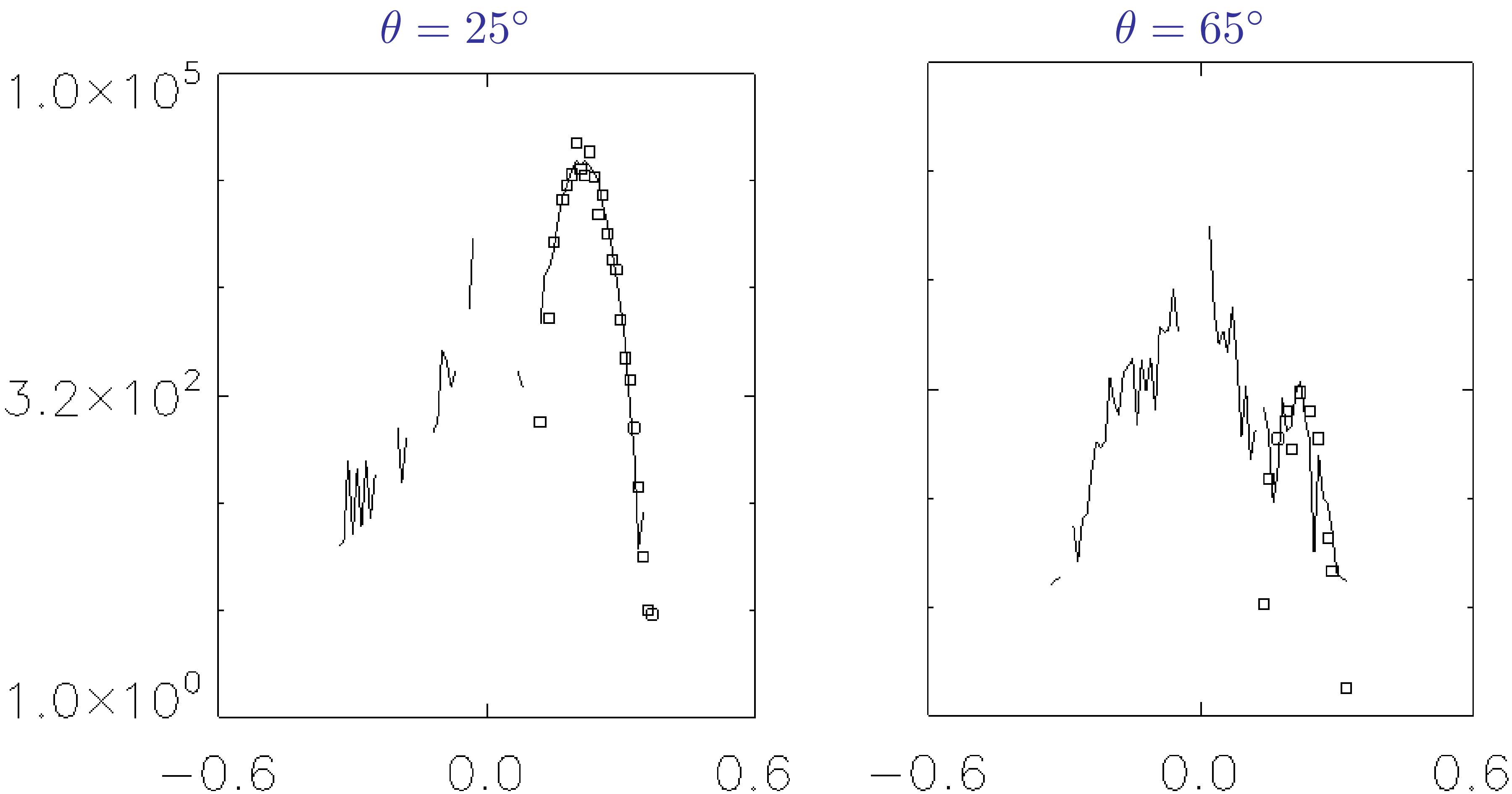

f(v/c) - Electron Distribution Functions at cut (a) : actual (−), mapped (◇).

Liouville Mapping

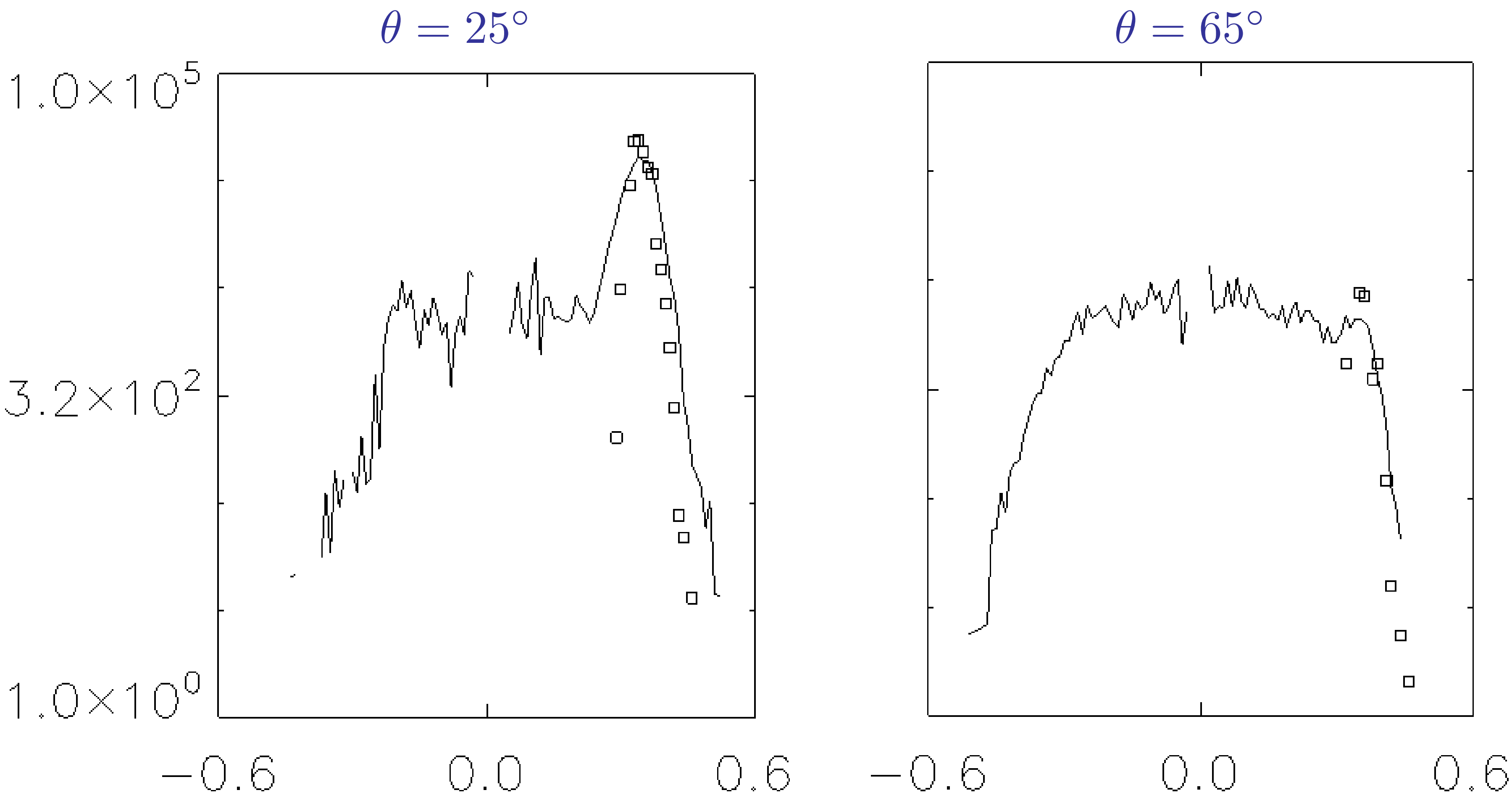

f(v/c) - Electron Distribution Functions at cut (b) : actual (−), mapped (◇).

Liouville Mapping

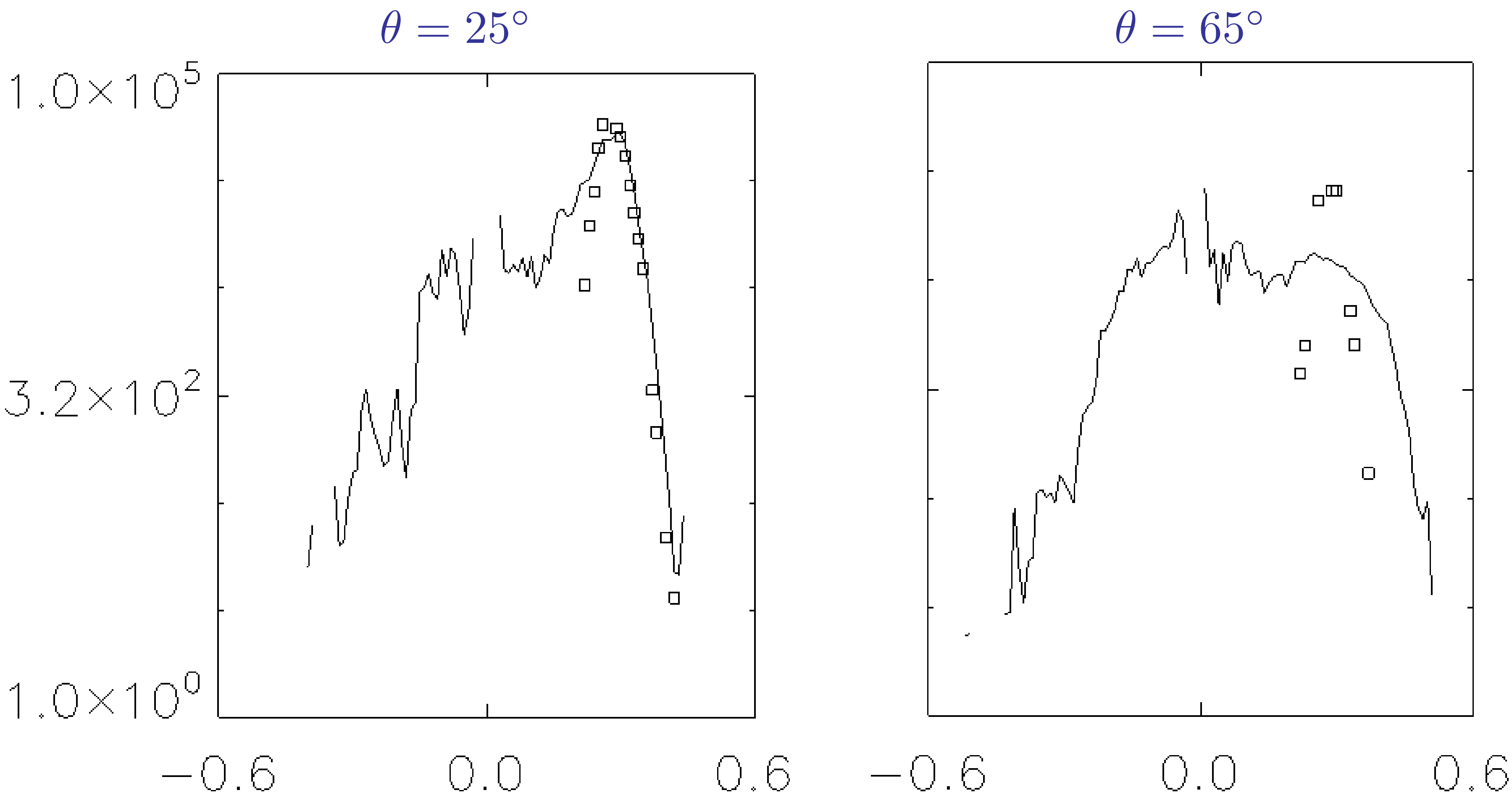

f(v/c) - Electron Distribution Functions at cut (c) : actual (−), mapped (◇).

Cross-Shock Potential Jump from Liouville Mapping

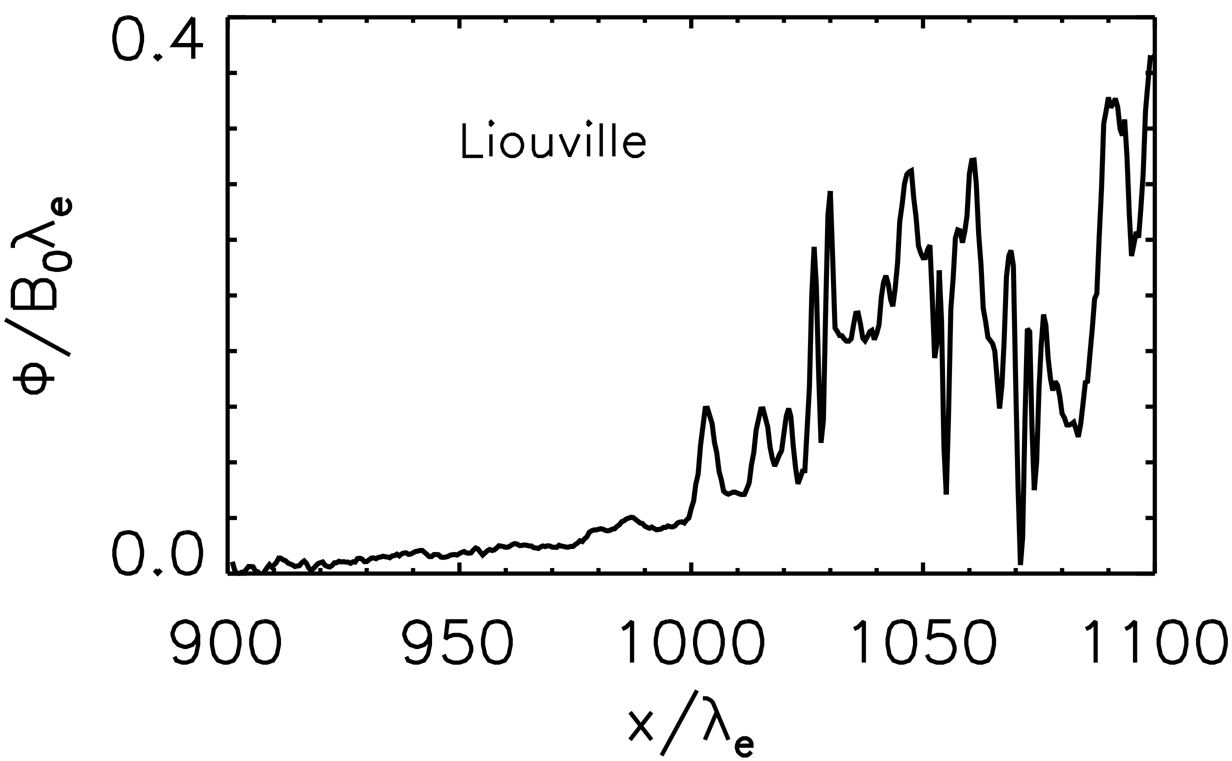

The cross-shock potential Φ_{LM} resulted from the Liouville mapping analysis in the deHoffmann-Teller frame.

Cross-Shock Potential Jump from Simulation

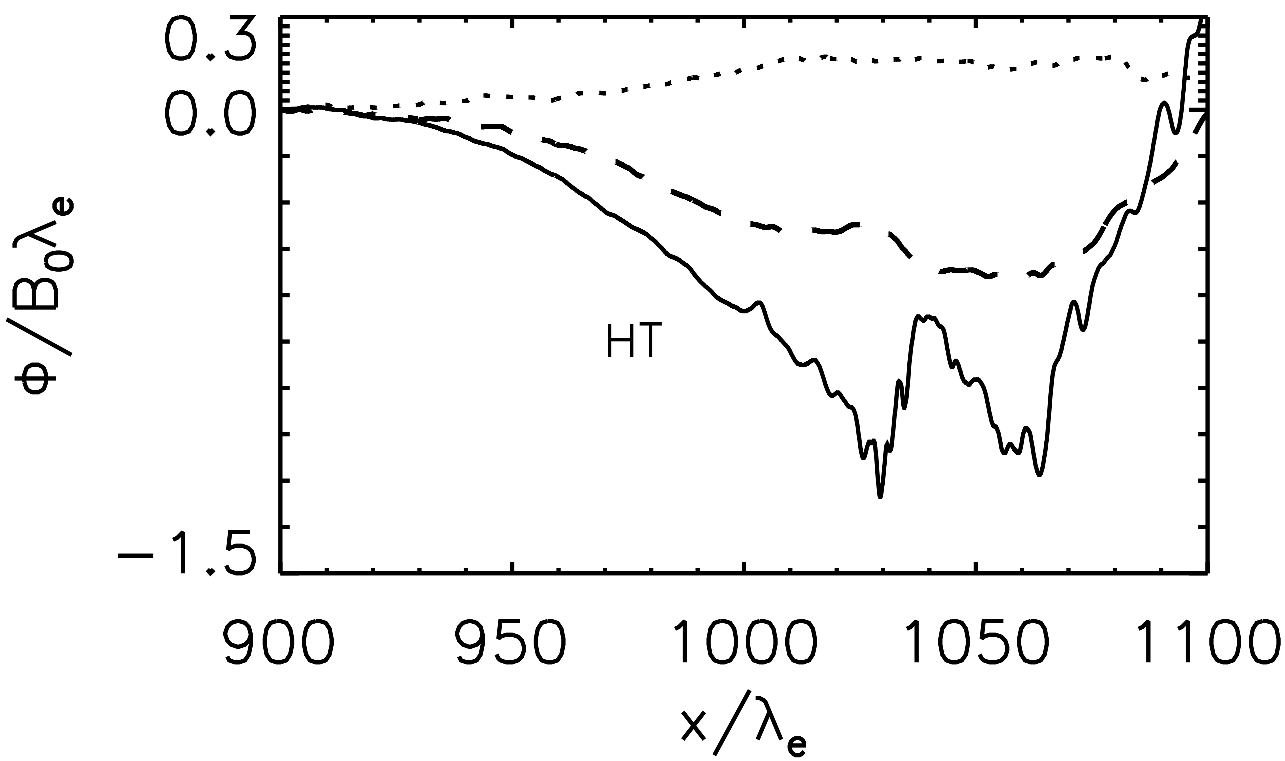

The integrated electric field in the deHoffmann-Teller frame: the potential along the Ox- normal direction (solid line), Oy (dashed), and Oz (dotted).

Exact Liouville Mapping

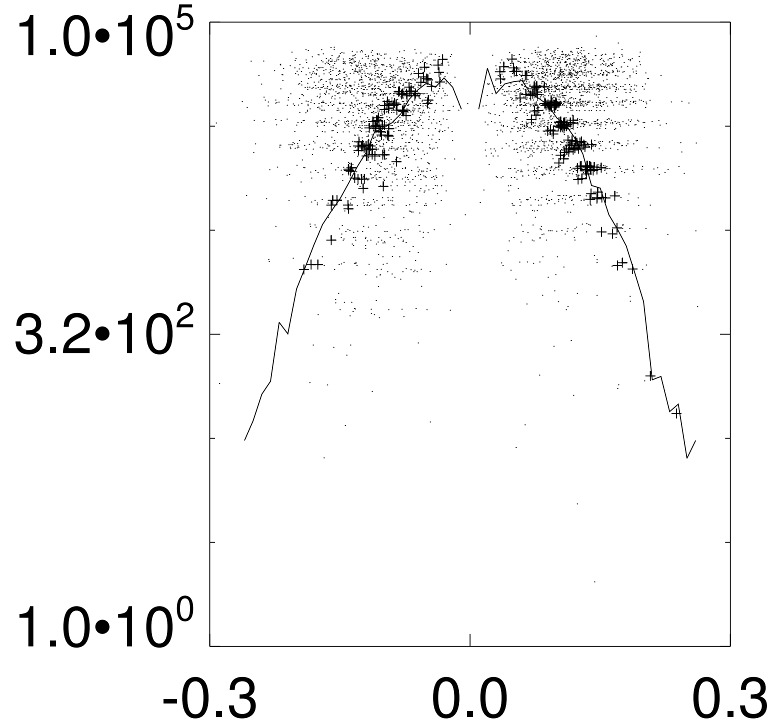

Result of the "exact" Liouville mapping applied on the adiabatic ("+") and non-adiabatic ("·") particles in the overshoot of the shock. The electron distribution function (solid line) is determined in the plasma rest frame at 90° pitch angle.

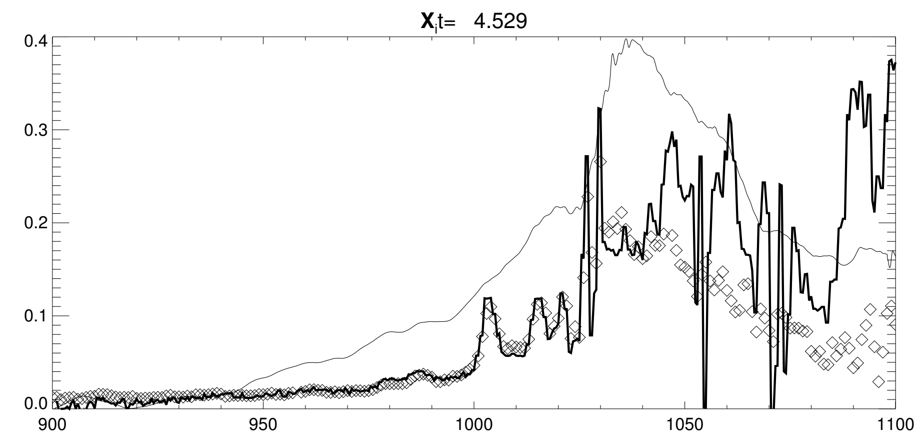

$\mathbf{X}_i$t= 4.529
0.4
0.3
0.2
0.1
0.0
900
950
1000
1050
1100

Summary

The electron distribution functions have been mapped at the foot, ramp and overshoot of a low beta quasi-perpendicular collisionless shock. The cross shock potential obtained by the PIC code is compared with the one obtained from the Liouville mapping method . The Liouville mapped estimations follow the trend of the electric field potential but deviations can be seen mostly behind the overshoot of the shock. A good agreement is noticed with the Goodrich and Scudder (1984) approximation in the foot and ramp regions. The discrepancies observed at the mapped distribution functions are mainly provided by: 1. Large inaccessible regions in the velocity space for the upstream incoming electrons and 2. the nonstationarity of the shock .

References

1. Lefebvre B., S. J. Schwartz, A.F. Fazakerley, and P. Decreau, Electron dynamics and cross-shock potential at the quasi-perpendicular Earth's bow shock, J. Geophys.Res., 112, A09212, 2007.
2. Goodrich C.C. and J.D. Scudder, The adiabatic energy change of plasma electrons and the frame dependence of the cross-shock potential

at collisionless magnetosonic shock waves, J. Geophys. Res., 89, A8, 6654-6662, 1984.
3. Hull A.J., J. D. Scudder, D.E. Larson and R.Lin, Electron heating and phase space signatures at supercritical, fast mode shocks, J. Geophys. Res., 106, A8, 15,711-15,733, 2001.